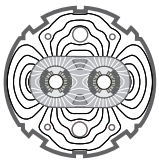

Preliminary draft 15:22 April 22, 2008

April 22, 2008

Estimation of BLM thresholds on the LHC Insertion Superconducting Magnets

Christine Hoa, Mariusz Sapinski *
CERN

Keywords: insertion region, quench prevention

Summary

Interaction Points of LHC machine are regions with elevated radiation. The first magnets after interaction point are subject of flux of debris from the interactions. In this note the IP 1 has been studied. An estimation of the residual signal in the Beam Loss Monitors due to the debris is made. In addition four beam loss scenarios on aperture limitations are considered. An estimation of Beam Loss Monitor signal corresponding to quench-critical energy deposition in magnet coils is made.

*mail: mariusz.sapinski@cern.ch

Contents

1 Introduction

The role of the magnets placed in the LHC insertion regions is to squeeze the beams and bring them to collisions at the interaction point. These magnets will be a subject of high heat loads due to debris from the interaction point (IP). Additinal beam losses on aperture limitations might be potentially more dangerous than for other magnets.

In this study the simulation of particle flux from IP and of beam loss in the magnet is made with FLUKA [1]. The particles of the hadronic shower are traced up to location of BLM monitors and they are stored in form of fluence as a function of energy for 7 types of particles: neutrons, protons, pions, gammas, electrons, positrons and kaons.

These fluences are convoluted with Beam Loss Monitor response function [3] in order to obtain the signal estimation in the chamber. This procedure allows to estimate the signal in the BLMs due to debris flux which will be a (permanent background) as well as additional signal from the beam losses on the aperture limitations of the magnets, which is potentially dangerous and might lead to quench.

2 Geometry description

All essential components in the insertion region up to 60 m from the interaction point have been implemented with a detailed description of their geometry, material and magnetic field. In the radial direction the components are included into the model up to 92 cm, corresponding to the positions of the Beam Loss Monitors (BLM). The BLMs are not described in details. Only the external envelops are implemented, in order to estimate the particle fluence entering every monitor.

The geometry has been described including details of the variations of the vacuum chambers along the insertion IR1. The layout includes the TAS absorber in front of the inner triplet (see the red box on the Figure 1), the inner triplet composed of 4 superconducting magnets Q1 and Q3 (MQXA) and Q2a and Q2b (MQXB), the corrector magnets (MCBX, MQSX, MCBXA) and a TAS B absorber between Q2b and Q3 ().

The complete FLUKA geometry consists of more than 250 different regions. The colors on the Figure 1 represent different materials.

Different magnet designs (the Japanese MQXA and the American MQXB) are implemented as well. Q1 and Q3 are 4 layer MQXA magnets (Figure 3) and Q2a and Q2b are 2 layer MQXB magnets (Figure 4). The coils are made of Nb-Ti cables, with slightly different composition depending on the type of magnet and layer position (K1 and K2 for MQXA, and F1 and F2 for MQXB, see [2]). The superconductor layers are separated by insulation material in G10. A thin kapton layer of 0.04 cm is placed between the magnet and the beam pipe in stainless steel. The beam screens are also implemented into the geometry. In IR1, the helium channels are positioned in the horizontal plane.

The coordinate system is the LHC coordinate system, ie. x-axis is horizontal,

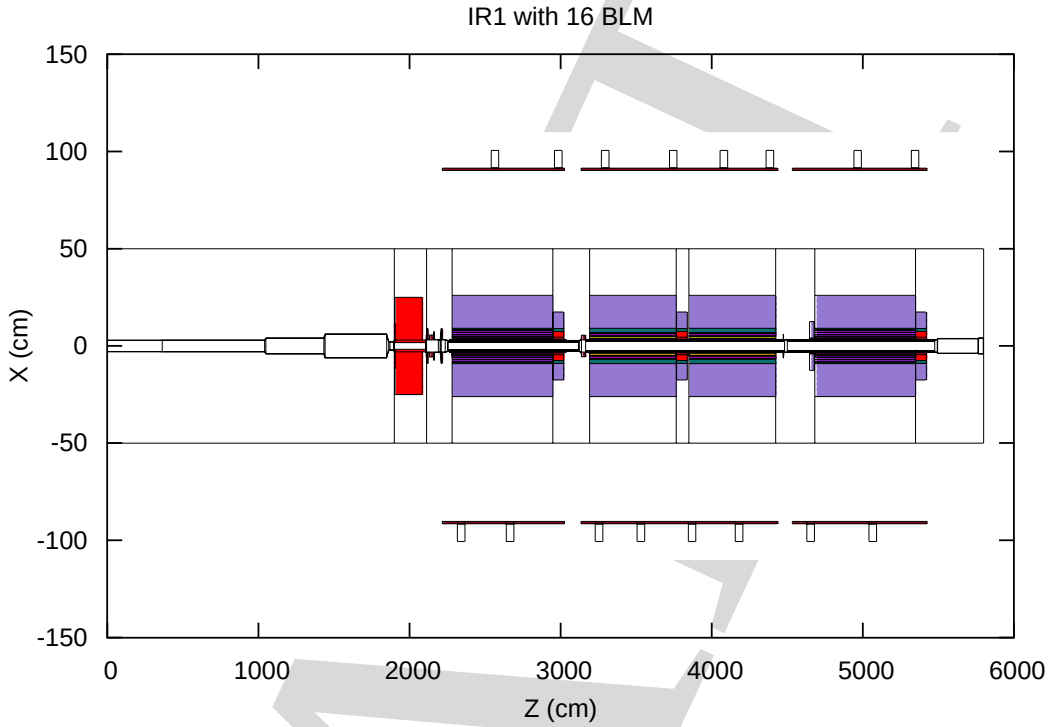

Figure 1: *Simulated geometry; the scales in z and x are different. The small boxes at* x = ±90 cm *designate 16 Beam Loss Monitors protecting the triplet magnets.* F:geom

transverse to the beam direction, y-axis is vertical and z is along the beams. The origin of the coordinate system is in the center of ATLAS detector. The beam B1 is the one coming from the IP and B2 is the one going towards IP.

3 Magnetic field

Detailed two-dimensional[1] magnetic field maps for the Japanese and American magnets and an analytic description of the solenoid field in the ATLAS detector region (2 Teslas) are taken into account in the model.

3.1 Quadrupole field

The quadrupole magnets have a peak field in the coils of 8.6 T (MQXA, Figure 2) and 7.7 T (MQXB, Figure 6). The 2 different magnetic field maps are calculated

[1]The change of the magnetic field in the z-direction is not simulated.

with ROXIE [4] and the nominal operating gradient is 203.716 T/m. The maps are 2D with no hard edge effects taken into account.

The sequence of the 4 quadrupoles is FDDF (F stands for Focusing and D for Defocusing), for beam 1 (protons travelling clockwise [5]). For the secondaries, the field sequence is also FDDF in the horizontal plane, for the positively charged particles, coming out from the IP1.

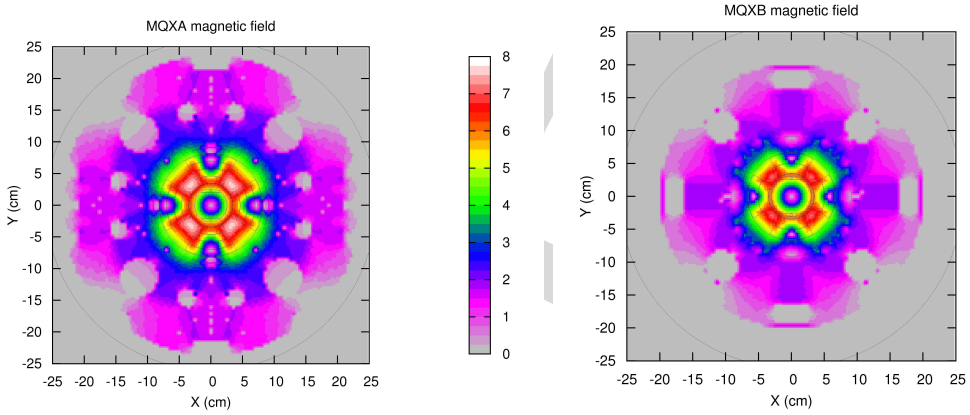

Figure 2: *Magnetic field of the MQXA and MQXB magnets (from Roxie).*

3.2 Solenoid field

In IR1 (ATLAS), the maximum solenoid field is 2 T. The fields are described analytically [5]. The effect of the solenoid becomes negligible (less than 0.2 T) 5 m after the IP (Figure 3).

4 Monte Carlo sample

Two kinds of Monte Carlo samples were needed to perform this study. First is the scenario where the debris from the intercation point hit the coils of the magnets. The second kind are 4 beam loss scenarios in the aperture limitations of the setup. 2 losses has been simulated at the entrance of the insertion region (1h, 1v), 2 at the end of the insertion region (2h, 2v).

4.1 Proton-proton debris

The event-generator used to simulate the proton-proton collisions at the center of mass energy of 14 TeV is DPMJET III, directly called from inside FLUKA. The parameters given in Table I applied for bunches description and are derived from the baseline beam parameters found in [5]. For IR1, the bunches have a vertical crossing plane with a half crossing angle of 142.5 μrad. The nominal luminosity is

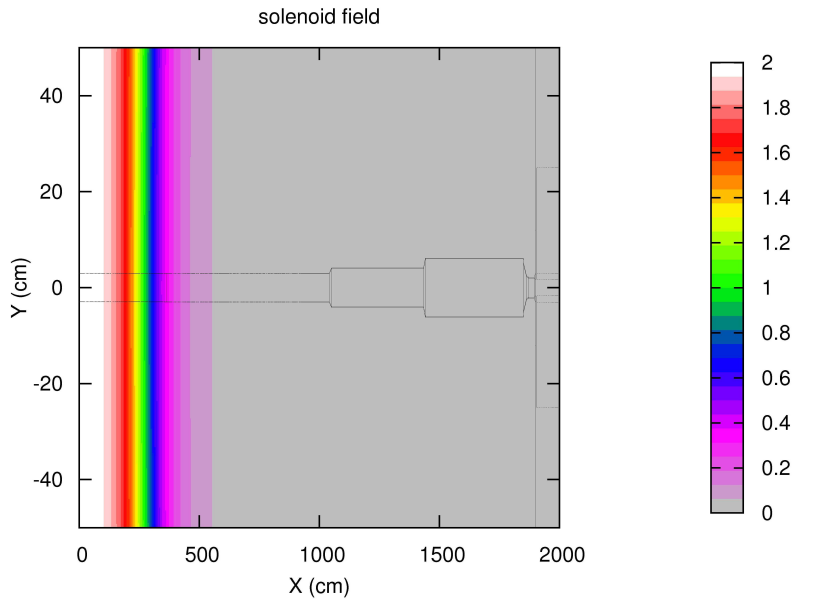

Figure 3: *Magnetic field of the ATLAS solenoid. Magnetic field intensity in Tesla.* F:SolenoidFiel

$L = 10^{34}\ s^{-1}cm^{-2}$ and the proton-proton cross section is 80 mbarn including inelastic scattering and single diffraction events.

p-p collisions	beam parameters IR1
Crossing angle plane	vertical
Half crossing angle (μrad)	142.5
P_x(GeV/c) beam1/beam2	0/0
P_y(GeV/c) beam1/beam2	$9.975 \cdot 10^{-1}/9.975 \cdot 10^{-1}$
P_z(GeV/c) beam1/beam2	$+7.0 \cdot 10^3/-7.0 \cdot 10^3$
$\sigma_x, \sigma_y(\mu m)$	11.81
σ_z(cm)	5.34
L, Luminosity($cm^{-2}s^{-1}$)	10^{34}
A, Cross section(mbarn)	80
statistics	17200

Table 1: *Beam parameters for the debris scenario.* T:beam_pars

4.2 Beam losses

Two geometrical aperture limitations has been considered in this study as the most probable locations of the beam losses. They are placed at two extremities of the triplet magnets. The other loss scenarios are not covered in this study.

For the beam loss scenarios, the source particles are mono energetic (7 TeV) proton beams in the z-direction, impacting a point in the insertion region, with a deviation angle of 240 μrad.

Two scenarios (1h, 1v) describe a proton beam in the positive z direction, i.e. entering the insertion region from the interaction point and impacting the insertion region before the magnet Q1. The two other scenarios (2h, 2v) describe a proton beam in the negative z direction, impacting the insertion region close to the magnet Q3. For each case, the impact point is in the horizontal plane (1h, 2h) or in the vertical plane (1v, 2v).

beam-loss scenarios	1h	1v	2h	2v
impact plane	horizontal	vertical	horizontal	vertical
No of simulated protons	1000	1000	1000	1000
energy (TeV)	7	7	7	7
impact point x (cm)	-2.12	0	2.62	0
impact point y (cm)	0	2.6	0	3.1
impact point z (cm)	2253.65	2253.65	5493.2	5493.2
impact angle (μrad)	240	240	240	240

Table 2: *Beam parameters for the beam loss scenarios.*

T:beam_loss_pa

In total five Monte Carlo samples has been generated for this study.

5 Energy deposition results

The Table 3 summarizes the peak energy density (ρ_E) deposition in the magnets for the five scenarios. The peak are calculated on a volume size corresponding to the inner cable ($3.5 < R < 4.61$ cm) section and a length of 2 cm in the z direction. For the four beam loss scenarios, the energy deposition is in $GeV/cm^3/proton$. In the case of the pp collisions, the energy deposition is given in $GeV/cm^3/collision$.

As expected, the peak occurs at the entrance of Q1 in the beam loss 1h scenario: Q1 is focussing the protons in the horizontal plane. For the beam loss 1v scenario, the spot center of proton beam is farther from the beam axis, due to the cooling channels in the horizontal plane (x=2.6 cm for 1v, x=-2.12 for 1h). The spot centre (z=2253.65 cm) is located before the Q1 magnet (which starts at z=2282.8 cm). Hence, the location of the peak is different in the R (transverse) and Z (longitudinal) directions. In addition the magnetic field of Q1 is defocusing in the vertical plane. (EXPLANATION TO BE CONFIRMED?)

scenario	mag	z (cm)	E_D $\frac{GeV}{cm^3}$	stat error (%)	E_D^{QL} trans. $\frac{mJ}{cm^3}$	P_D^{QL} steady st. $\frac{mW}{cm^3}$
1h	Q1	2302	3.92	1.7	1.2	12
1v	Q1	2436	4.06	2.6	1.2	12
2h	Q3	5315	0.67	4.6	1.2	12
2v	Q3	5318	1.51	2.3	1.2	12
pp debris	Q1	2891.0	$2.73 \cdot 10^{-2}$	5.9	1.2	12

Table 3: *Maximal energy density depositions ρ_E for different beam loss and pp-debris scenarios. The Quench Levels E_D^{QL} for fast losses are from Darek [2]. Steady State QL are are from Mokhov [7].*

T:edeps_max

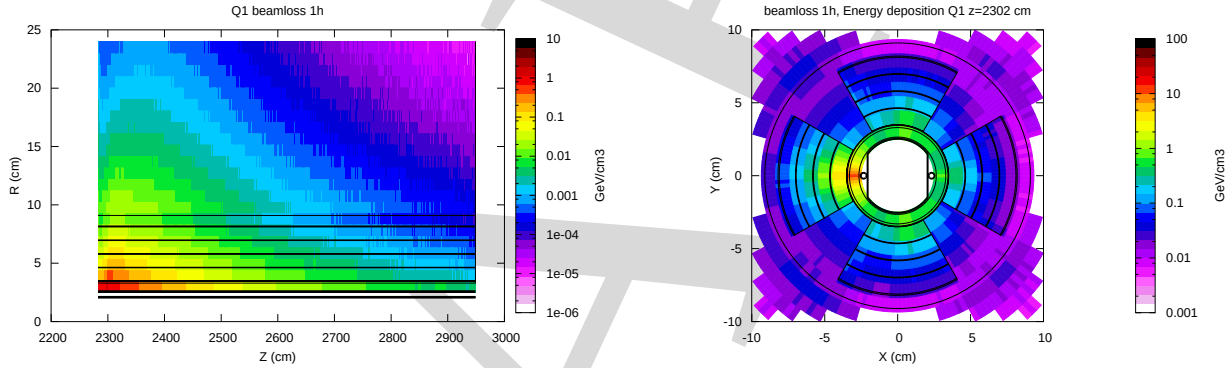

Figure 4: *Energy deposition in the coil in case of beam loss* 1h. *Left plot shows distribution integrated over ϕ and the right one integrated over length of Q1 magnet.*

F:1h_edp

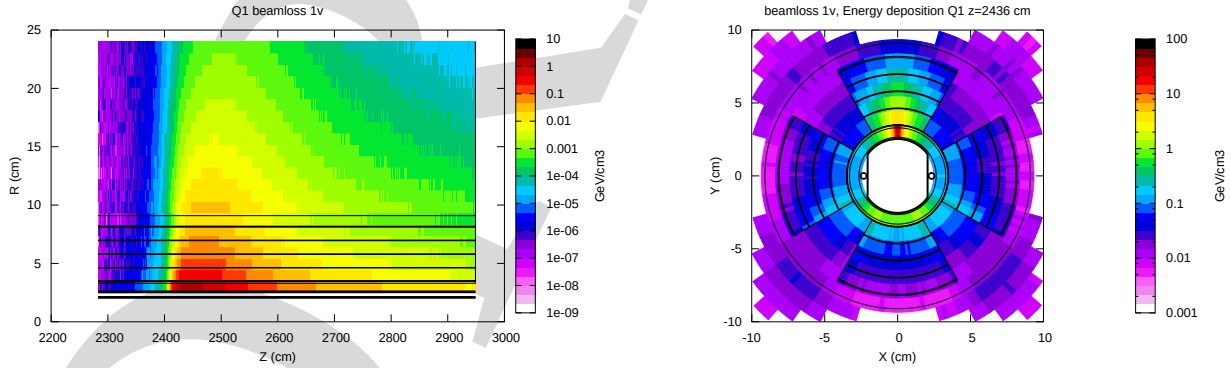

Figure 5: *Energy deposition in the coil in case of beam loss* 1v. *Left plot shows distribution integrated over ϕ and the right one integrated over length of Q1 magnet.*

F:1v_edp

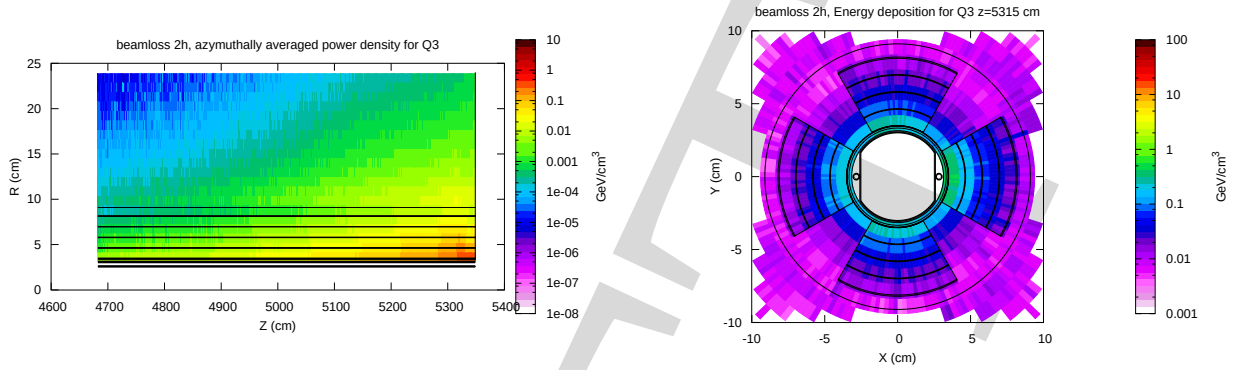

Figure 6: *Energy deposition in the coil in case of beam loss* 2h. *Left plot shows distribution integrated over ϕ and the right one integrated over length of Q3 magnet.* F:2h_edp

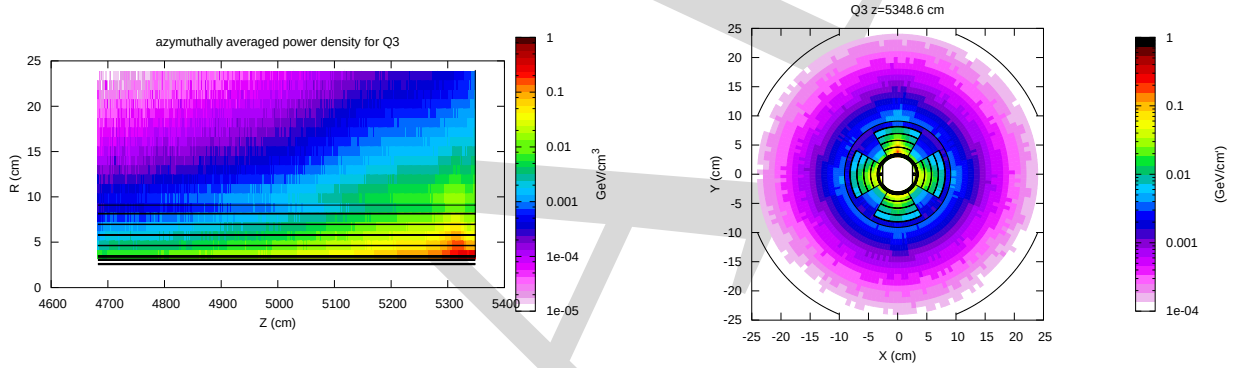

Figure 7: *Energy deposition in the coil in case of beam loss* 2v. *Left plot shows distribution integrated over ϕ and the right one integrated over length of Q3 magnet.* F:2v_edp

6 Signals in the BLMs

The signals in the BLMs are estimated by multiplying the flux registered at the sufrace of the BLMs with the response functions obtained Markus [3]. The response functions exists for particles hitting monitors at angles $\phi = 0°$, $30°$, $60°$and $90°$, where $\phi =$ is the angle between monitor axis and the momentum vector of impacting particle. An example of the response functions for particles hitting the BLM at $30°$are presented on the left plot of Figure 9.

The function used is chosen according to mean value of the angular distribution of particles hitting the monitor (Figure!). Functions for $30°$and $60°$give result different by xx%.

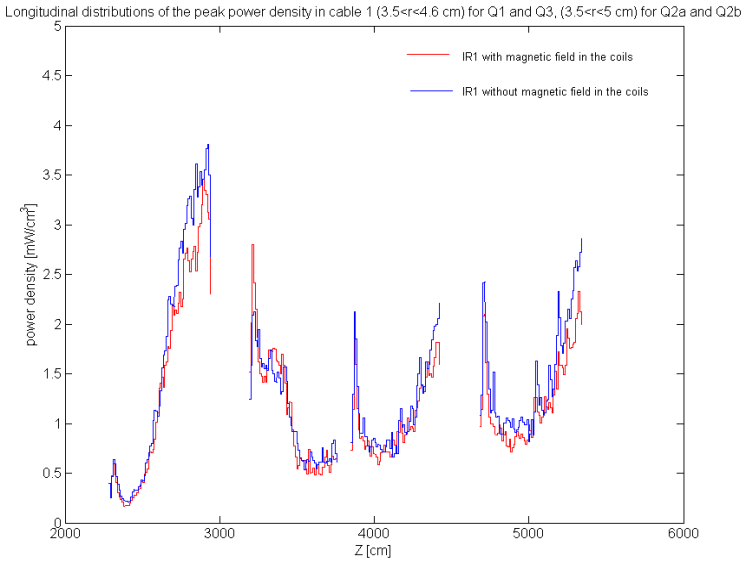

Figure 8: *Longitudinal distribution of the peak power density in the inner cable of insertion magnets due to flux of pp-interaction debris (from [6]) The gaps along the curves correspond to spaces between magnet coils.*

Christine

F:fromChFig28

6.1 Debris from IP

Here it is estimated what is the signal produced in BLM monitors due to the background from the IP.

The debris from the IP will come in pulses every 25 ns. These pulses are seen in the BLMs as a constant current (I_{pp}). This current can be estimated from Equation 1.

$$I_{pp}[A] = Q_{pp}[C] \cdot L[cm^{-2}s^{-1}] \cdot A[cm^2] \quad (1)$$

E:debris_curre

In this Equation L is the luminosity assumed to be the nominal LHC luminosity $10^{34}cm^{-2}s^{-1}$ and the cross section A is 80 millibarns ie. $8 \cdot 10^{-26}$ cm^2. This conditions lead to about 20 proton-proton interactions in the IP per bunch-crossing. The Q_{pp} is charge collected on the BLM per one proton-proton interaction. The results of the simulation are presented in Table 4.

Using values of charge collected on the chamber due to single pp-interaction (Q_{pp}), one can find out that the highest current is 216 nA in the BLM number 5, down to 47.2 nA for the last BLM. This current will be clearly visible in the signals from the BLMs (1000 times more than the 10 pA offset current, which is always present in electronics in order to provide a continuous test).

This signal corresponds to peak power density of about 4 mW/cm^3 while the quench limit of the cable is about 12 mW/cm^3.

The maximum signal is observed in the BLM number 5 which is 3.6 meters after the maximal energy deposit in the coil. The signal in the BLMs is mainly produced

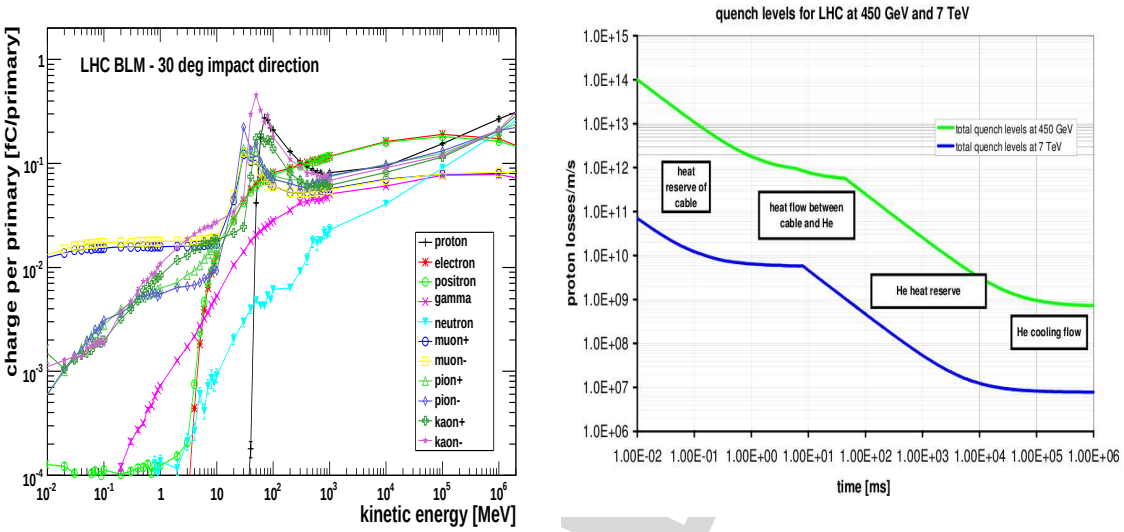

Figure 9: *Left plot: response function for particles hitting the BLM at 30 deg. Right plot: Quench level as a function of beam loss duration (based on [9]).*

F:resp_fction

Note044

by gammas (40-50%), then there is large contribution from pions (up to 20%), from electrons (up to 20%) and from positrons (up to 15%). The signal composition weakly depends on BLM location.

The spectrum of particles from the debris hitting the BLMs is in general harder then the one from beam losses. For instance in case of BLM 1 the fraction of the fluence with energies above 10 MeV is 11% in case of debris and 7% in case of loss 1h. The 10 MeV is the region where the BLM response functions rise significantly.

6.2 Beam losses

Four configurations of beam loss has been considered. The losses are most likely to happend at the beginning (z=2253.65 cm) and at the end (z=5493.2 cm) of the triplet magnet. In addition, for every of this location, a loss in horizontal and in vertical plane is considered.

In the Figure 10 a particle fluence for loss in horizontal in the first location for the first BLM is plotted. The flux is dominated by neutrons and gammas. These fluxes are similar to the ones obtained by Geant 4 simulations of LHC magnets (plot) [7].

ThresholdNote

In the Table 4 the charges collected in each BLM chamber which correspond to one lost proton ($Q_{loc} = Q_{1v}$ or Q_{1h} or Q_{2v} or Q_{2h}) are presented.

The maximum of the signal is observed usually in the monitor which is the closest to the loss location, except of loss 1v for which the first monitor is located before the cascade reaches the cryostat radius.

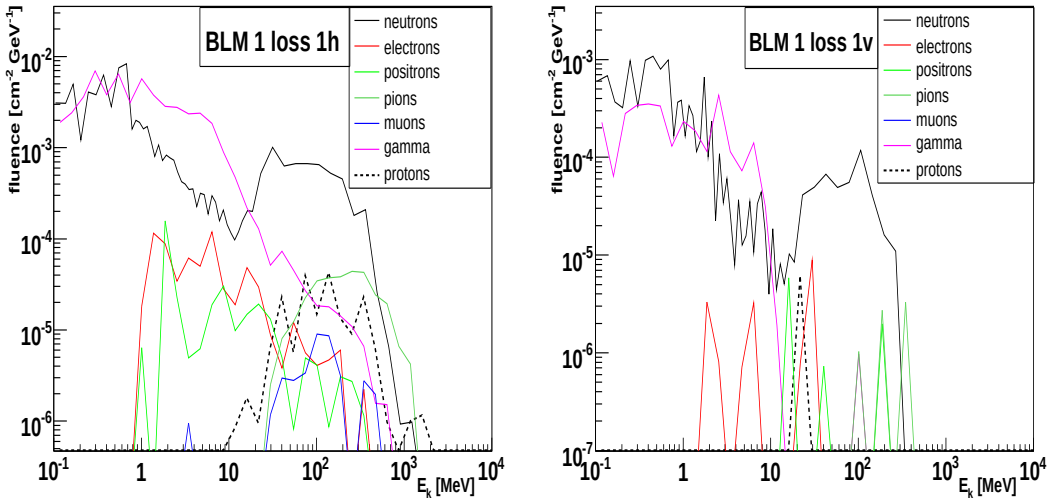

Figure 10: *The fluence of the particles entering the first Beam Loss Monitor in case of beam loss at 2253.65 cm from the IP1. On the left plot the loss is in horizontal plane, on the right one in the vertical.*

u_blm1_loss1h

In general in the shower maximum there is a variety of particles contributing to the signal, while in the tails the main contribution comes from gammas and pions (for losses 2h there is also a significant contribution from protons). Neutrons give relatively weak detector response therefore, even if they are main contribution to the spectrum, they do not contribute to the final signal in the chambers.

7 Estimation of quench-preventing thresholds

7.1 Fast losses

The energy to quench the magnet in case of fast losses is almost three order of magnitude larger than for steady-state losses. Therefore the quench level for fast beam loss is independent of the steady energy flux coming from the pp-debris.

In order to estimate the quench level for fast losses first the number of protons lost which will provoke the quench must be calculated from Equation 2.

$$N_p^{QL} = E_D^{QL}/E_D \tag{2}$$

E:Qprot

Then the threshold in the corresponding BLMs is obtained by multiplying the signal form a single proton by number of protons as in Equation 3, where Q_{loc} corresponds to charge collected in a monitor for loss location loc, which can be 1v, 1h, 2v or 2h.

$$Q^{QL} = Q_{loc} \cdot N_p^{QL} \tag{3}$$

E:QLfast

The threshold can be expressed in Greys using Equation 4.

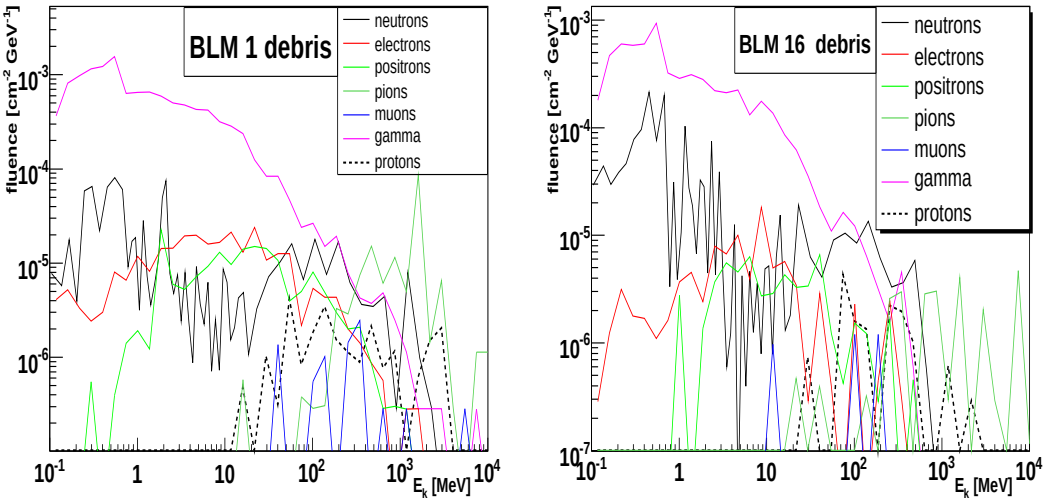

Figure 11: *The fluence of the debris particles from the IP entering the first and the last Beam Loss Monitor.*

F:flu_debris

$$D[\mathrm{Gy}] = Q^{QL}[\mathrm{C}]/5.4 \cdot 10^{-5}[\mathrm{C/Gy}] \quad (4)$$

E:QLGy

where the conversion constant $5.4 \cdot 10^{-5}[C/Gy]$ has been calcualted by Bernd [10].

In Table 5 the BLM signals corresponding to quench-level losses are presented. As expected the BLMs number 1 and 2 protect Q1 magnet. The first monitors does not see the signal from vertical losses, but putting similar threshold on BLMs 1 and 2 should protect from fast losses on the first aperture limitation before the triplets looking from IP.

The thresholds for the second location of the beam loss are significantly higher. It can be explained by lack of material seen by particles coming from this direction.

7.2 Steady-state losses

In case of steady-state losses the Quench Level of the MQXA magnet is about 12 mW/cm^3 Mokhov [?]. The maximal energy density deposited by debris of pp interaction in the magnet is $2.73 \cdot 10^{-2}$ GeV/cm^3 $= 4.37 \cdot 10^{-9}$ mJ/cm^3 per interaction (see Table 3). The maximum is located close to the end of the Q1 magnet. For nominal LHC beam intensity the deposited power density in maximum is 3.5 mW/cm^3, i.e. only 4 times below the Quench Level.

The beam losses in the triplet magnets are limited by the power already deposited by the pp-debris. The rate at which protons can be lost in order to quench the magnet can be expressed by Equation 5, where P_D^{QL} is the power density of steady-state Quench Level for the magnet and P_D^{pp} is the power density produced by pp-debris. As the maximum of the beam loss is well localized then the P_D^{pp} value is taken for the position of the maximum of beam loss (maximum location is shown in the 3rd column of Table 3).

BLM No	dcum [m]	z [cm]	protected magnet	signal per proton Q [aC]				
				Q_{pp}	Q_{1h}	Q_{1v}	Q_{2h}	Q_{2v}
1	26635.46	2343	Q1	169.1	553	24	0.0	2
2	26633.22	2566	Q1	109.6	268	511	0.5	2
3	26632.22	2666	Q1	124.8	135	321	0.3	7
4	26629.03	2985	Q1	131.0	26	41	4.8	24
5	26626.33	3255	Q2a	270.0	23	63	0.2	1
6	26625.93	3295	Q2a	256.0	24	74	0.0	3
7	26623.57	3531	Q2a	148.0	19	24	3.5	5
8	26621.43	3745	Q2a	69.8	1	2	3.3	156
9	26620.18	3870	Q2b	83.7	2	3	18.7	33
10	26618.07	4081	Q2b	61.6	1	3	44.8	39.6
11	26617.07	4181	Q2b	74.5	1	0.1	108.0	67.9
12	26615.03	4385	Q2b	71.0	0	0	43.2	89
13	26612.33	4655	Q3	183.2	0	4	45.6	39
14	26609.22	4966	Q3	91.6	0	1	76.7	163
15	26608.22	5066	Q3	145.7	0	0	190.4	174
16	26605.42	5346	Q3	59.0	0	0	2907.5	1839

Table 4: *Summary of signals in BLMs, corresponding to one lost proton (*1h, 1v, 2h, 2v*) or for one bunch crossing in the IP (pp). The second column shows the dcum of the middle of every BLM as on the integration drawing L0272343PL [8].* integration_webpage T:summary2

$$R_p^{QL} = (P_D^{QL} - P_D^{pp})/E_D \quad (5)$$ E:Nprot_ss2

In case of loss location 1v and 1h the location of the loss maximum is in region where pp-debris deposits very small amount of energy (see Figure 8) therefore it is assumed that $P_D^{pp} = 0$. For instance for loss location 1h the quench is provoked by loss of about $R_p^{QL} = 1.9 \cdot 10^7$ protons per second what corresponds to only one lost protons every second bunch.

In case of losses 2v and 2h the power density from debris is about $P_D^{pp} = 1.8$ mW/cm^3 which is 7 times below the Quench Level. It reduces the power density margin form 12 mW/cm^3 to about 10 mW/cm^3.

To calculate the quench-preventing threshold in the BLM a sum of fluxes from pp-debris and from beam losses must be taken. For nominal LHC collision rate it is expressed by Equation 6.

$$I^{QL} = Q_{pp}LA + Q_{loc}R_p^{QL} \quad (6)$$ E:SS1

It can also be expressed in terms of dose rate using Equation 4.

In Table 6 the quench-preventing thresholds for steady-state losses are presented. In the last column a contribution to the quench-like signal from debris is shown:

scenario	protons to quench N_p^{QL}	BLM No	BLM signal		
			nC	Gy	Gy/s
1h	$1.91 \cdot 10^6$	1	1.06	$1.96 \cdot 10^{-5}$	0.49
1v	$1.85 \cdot 10^6$	2	0.95	$1.76 \cdot 10^{-5}$	0.44
2h	$1.12 \cdot 10^7$	16	32.6	$6.04 \cdot 10^{-4}$	16.0
2v	$4.96 \cdot 10^6$	16	9.1	$1.69 \cdot 10^{-4}$	4.23

Table 5: *Values of the signal in the selected BLMs corresponding to quench energy deposition. The last column presents quench level in* Gy/s *for the shortest signal integration time of* 40 μs.

T:qthresholds

$f_{pp} = \frac{Q_{pp}LA}{Q_{pp}LA+Q_{loc}R_p^{QL}}$. For losses 1h and 1v a small increase of the signal from the pp-debris constant background - by only a few percent - has a meaning of the reaching the quench level. Therefore maybe different BLMs should be used to protect Q1 from losses 1v and 1h.

scenario	protons per sec to quench (R_p^{QL})	BLM No	BLM signal			f_{pp}
			nA	Gy/s	mGy	
1h	$1.9 \cdot 10^7$	**1**	145.8	$2.7 \cdot 10^{-3}$	3.5	0.93
1h	$-\|-$	2	92.8	$1.7 \cdot 10^{-3}$	2.2	0.94
1v	$1.25 \cdot 10^7$	2	94.1	$1.7 \cdot 10^{-3}$	2.2	0.93
2h	$9.5 \cdot 10^7$	**16**	323.4	$6.0 \cdot 10^{-3}$	7.8	0.15
2h	$-\|-$	15		$6.0 \cdot 10^{-3}$		
2v	$4.2 \cdot 10^7$	16	124.4	$2.3 \cdot 10^{-3}$	3.0	0.38

Table 6: *Values of the signal in the selected BLMs corresponding to quench-provoking power deposition in the coil. The 6th column presents signal integrated over 1.3 second. The last column presents the fraction of signal from pp-debris in the total monitor signal at the quench level. The monitors marked with bold font are the ones most sensitive for the given loss.*

T:qthr_ss

In case of losses 2h and 2v the last BLM is well placed to detect losses and to protect Q3 magnet.

7.3 Estimation of errors

The following error sources enter into estimated values of quench-preventing thresholds:

- accuracy of the simulation of the hadronic cascade tail,
- accuracy of the geometry implementation,

- accuracy of the simulation of the detectror response function,
- error made by choice of the response function corresponding to a single, average angle of particles.

8 Conclusions

The results of the study are the Beam Loss Monitors thresholds to protect triplet magnets in IP1 against quenching. The two most probable beam loss locations at the beginning and at the end of the triplet complex are considered together with constant energy flux from pp-debris from IP.

It has been found that for fast losses the BLMs number 1 and 2 protect against losses from location 1 (aperture limitation between triplet magnet and IP). The threshold values should be of the order of $1.7 \cdot 10^{-5}$ Gy. In case of losses due to incoming beam the thresholds are significanltly higher due to (probably) much less material between loss locations and BLM number 16. The thresholds are expected to be about $6 \cdot 10^{-4}$ Gy for horizontal loss and $1.7 \cdot 10^{-4}$ Gy for vertical loss.

This thresholds can be compared to the ones in Tevatron [13] which are about $7 \cdot 10^{-5}$ Gy for fast losses.

In the case of steady state losses the same BLMs give the largest signal. For the losses in the location 1v and 1h the thresholds are determined to be at the level of $1.7 - 2.7 \cdot 10^{-3}$ Gy/s but the sensitivity of the BLMs itself to the loss is very small because more than 90% of quench-level signal comes from pp-debris. Therefore in order to protect magnet from quench a very small variation of the signal (of the order of percent) must be detected. It is not possible to set on these monitors a safety margin of a factor of a few, because they would dump the beam during normal operation. It is worth noticing that presence of substantial flux of praticles from normal accelerator operation modify the dependence of the loss as a function of time presented on the right plot of Figure 9.

In case of loss location 2h and 2v the thresholds should be set to $6 \cdot 10^{-3}$ Gy/s and $2.3 \cdot 10^{-3}$ Gy/s respectively. Here most of the signal in BLM comes from beam losses.

The two scenarios presented here to not drain all possible loss locations therefor they can be used to set up thresholds for BLMs number 1,2 and 16 only. The thresholds of neighbour BLMs can be also estimated from this study (3 and 15,14). To set up thresholds for other BLMs on Q1 additional simulation of loss in aperture limitation between Q1 and Q2 is needed. For the rest of the BLMs simulations are needed on the magnet interconnections.

References

Fluka [1] A. Fasso, A. Ferrari, J.Ranft and P.R.Sala, "FLUKA: a multi-particle transport code", CERN-2005-10, INFN/TC-05/11, SLAC-R-773

Darek [2] D. Bocian in minutes of TOTEM meeting 2006.04.19

Markus [3] A. Stockner, PhD thesis

Roxie [4] S. Russenschuck, '1st International Roxie Users Meeting and Workshop - ROXIE : routine for the optimization of magnet X-sections, inverse field calculation and coil end design', CERN yellow report 99-01, 1999.

LHCDesing_I [5] 'LHC Design report, Vol. I The LHC main ring', CERN-2004-003, June 2004

Christine [6] Ch. Hoa, F. Cerutti, "Energy Deposition in the LHC Insertion regions IR1 and IR5", AT-MCS Note 2007...

ThresholdNote [7] A. Priebe, M. Sapinski, repport in preparation

ration_webpage [8] http://lhc-div-miwg.web.cern.ch/lhc-div-miwg/Plans_BLM/S12/Table_S12.htm

Note044 [9] J.B. Jeanneret, D. Leroy, L. Oberli, T. Trenkler, "Quench levels and transient beam losses in LHC magnets". LHC Project Report 044.

Bernd [10] B. Dehning, priv. communication

Bock [11] R.K. Bock et al., "Parameterization of the longitudinal development of hadronic showers", Nucl. Instrum. Meth. Phys. Res. 186 (1981) 533.

G4discussion [12] Alexander Howard, Gunter Folger, priv. communication

DStill [13] D.Still, presentation at LHC Collimation WG, 2005-04-15

HadG4 [14] J. Apostolakis, G. Folger, V. Grichine, A. Howard, V. Ivanchenko, M. Kossov "Hadronic Shower Shape Studies in Geant4", CERN-LCGAPP-2007-02